

ARMY RESEARCH LABORATORY



Nonlinear Behavior of Zn:Tetrabenzporphyrin

by Gary L. Wood, Mary J. Miller, and
Andrew G. Mott

ARL-TR-1229

January 1998

19980303 082

DTIC QUALITY INSPECTED 3

Approved for public release; distribution unlimited.

The findings in this report are not to be construed as an official Department of the Army position unless so designated by other authorized documents.

Citation of manufacturer's or trade names does not constitute an official endorsement or approval of the use thereof.

Destroy this report when it is no longer needed. Do not return it to the originator.

Army Research Laboratory

Adelphi, MD 20783-1197

ARL-TR-1229

January 1998

Nonlinear Behavior of Zn:Tetrabenzporphyrin

by Gary L. Wood, Mary J. Miller, and Andrew G. Mott
Sensors and Electron Devices Directorate

[DTC QUALITY INSPECTED 3]

Approved for public release; distribution unlimited.

Abstract

The nonlinear transmission of Zn:tetrabenzporphyrin was measured in a Z-scan setup with 532-nm wavelength laser light and a 13-ns pulse duration. The excited-state absorption cross section, the excited-state refractive index cross section, and the linear and nonlinear absorption contribution to a thermal index change were investigated. The effects of fluorescence and acoustic waves on the nonlinear response of TBP have been determined. Limiter performance was modeled in an $f/14$ limiter, and saturation effects were identified.

Contents

1. Introduction	1
2. Previous Results	2
3. Current Experiments	3
4. Results and Discussion	6
5. Conclusions	8
Acknowledgments	8
References	8
Distribution	9
Report Documentation Page	11

Figures

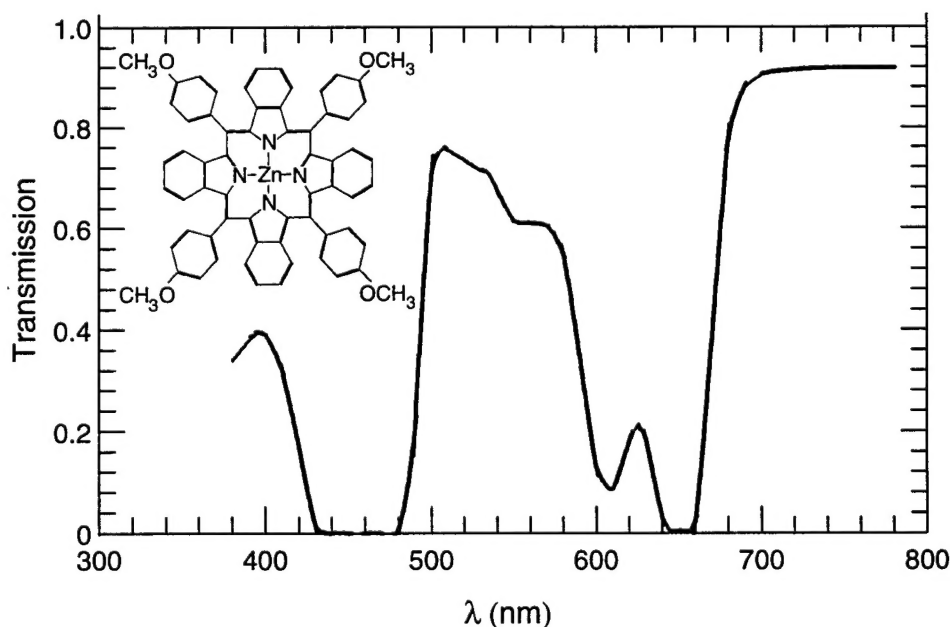
1. Transmission spectrum of Zn:meso-tetra (p-methoxyphenyl) tetrabenzporphyrin (TBP), taken in a 1-mm sample with a concentration of 0.5 g/l	1
2. $f/64$ limiter performance	2
3. Three-level model used to describe Zn:TBP	4
4. Typical open-apertured Z-scan	5
5. Open-apertured Z-scan for a saturated condition	6
6. $f/14$ limiter performance	7

1. Introduction

Programs in nonlinear optical (NLO) materials generally aim at developing materials that exhibit good optical quality, high damage thresholds, large nonlinear behavior, and fast response times, and that lend themselves to easy, low-cost manufacture. Many material systems have been investigated, but organic molecules offer perhaps the greatest challenge. In addition to the sheer size of this group of materials, many of the nonlinear processes that occur with these materials are not well understood. Despite these obstacles, organic molecules are attractive for a number of reasons. They are potentially low cost and easy to synthesize. They can often be incorporated into polymers or tailor-made for specific device designs. Further, organics have exhibited some of the largest nonlinear optical responses yet found.

An important class of organic NLO materials is that of organometallic materials, such as the phthalocyanine and porphyrin materials. These materials, which contain metals surrounded by highly conjugated π -bonds, can exhibit large nonlinear responses. Previous investigators have noted that the response of an organometallic material to wavelength, as well as its nonlinear magnitude, can be modified by variation in the metal atom that resides in the center of the molecules [1] or in the constituents attached to the macrocyclic ring. In this report, we highlight the nonlinear optical behavior of porphyrin-type organometallic materials, specifically, Zn:meso-tetra(p-methoxyphenyl) tetrabenzporphyrin (TBP) (fig. 1).

Figure 1.
Transmission spectrum of Zn:meso-tetra (p-methoxyphenyl) tetrabenzporphyrin (TBP), taken in a 1-mm sample with a concentration of 0.5 g/l. Transmission at 532 nm is 71.6%.



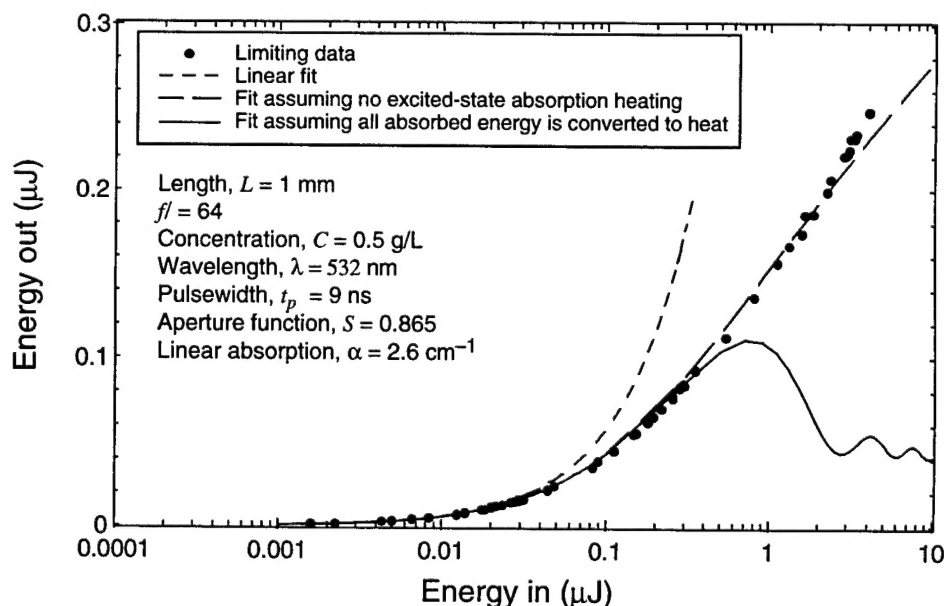
2. Previous Results

Earlier studies on TBP reported a second order hyper-polarizability, $|\langle\gamma\rangle_s|$, of 4.8×10^{-30} esu at 532 nm with picosecond pulses [2]. Other researchers have shown that the nonlinear transmission in TBP is fluence dependent and that the dominant nonlinear mechanism is excited-state absorption [3]. The same mechanism has been found in other porphyrin-type molecular systems [4].

In our previous investigations at 532-nm wavelength and ~10-ns pulse duration [5], we found that TBP has one of the largest reported excited-state absorption cross sections ($\sigma_{es} \sim 240 \times 10^{-18}$ cm²) and excited-state to ground-state cross-section ratios (~28), and that the index change at 532-nm is due to the contribution of thermal effects and an excited-state population. Because the excited-state refractive component, σ_r , was found to be negative, its effect was added to the thermal density change (which is also negative); this result is unlike previously reported results in macrocyclic organometallics. We have also shown [6] that TBP performs well when compared to similar organometallic materials and carbon black suspensions (CBS) in an $f/5$ optical limiting configuration. The TBP for the earlier study [6] and the work reported here was dissolved in tetrahydrofuran (THF) at a concentration of $C = 0.5$ g/l (where $\alpha_{532\text{ nm}} = 2.4$ cm⁻¹).

In our previous work, we measured the limiting behavior of TBP with the sample placed at focus in an $f/64$ optical system; this location corresponds to a spot size (half width e^{-2} maximum) at focus, w_0 of 21.4 μ m. The transmitted energy versus the input energy was measured through an apertured detector set to collect only the $1/e^2$ cone of the output Gaussian spatial profile energy (86.5 percent). We used parameters determined from a Z-scan analysis to model the limiter performance of this material. The limiting data (points) and the theoretical fits (curves) are shown in figure 2. The three curves indicate linear behavior (dashed line), the theoretical fit

Figure 2. $f/64$ limiter performance.



assuming that all the absorbed energy was converted into heat (solid line), and a theoretical fit assuming that only the energy from the linear absorption was converted into heat (long dashed line). The data were found to fit the latter model up to an input energy of $\sim 3 \mu\text{J}$, at which point the analysis broke down. As can be seen from the theoretical fits, the best limiting occurs when all the absorbed energy can be converted into heat. The data did not fit the best-case scenario (solid line), possibly because of other contributions not accounted for in this model, such as fluorescence, higher level transition states, material impurities, breaking of molecular bonds, saturation, boiling, or the acoustic wave not fully propagating across the beam during the length of the pulse. We explore several of these scenarios in this report and determine the most likely explanation.

3. Current Experiments

Although two effects are causing nonlinear transmission (nonlinear absorption and self-defocusing), the theoretical heating solid curve in figure 2 is all self-defocusing. Energy is not reaching the detector because a portion of it is spread over such a spot size that it cannot fit through the aperture about the f -cone, as it could at low input energies. Heating causes self-defocusing by changing the index of refraction. The incident radiation is absorbed by the TBP, and this energy is returned as heat, which increases the temperature of the surrounding THF solvent. The heated solvent then changes density, which in turn changes the index of refraction. Since the density is decreased, the index is decreased, so that the material forms a highly aberrated negative lens.

We confirmed the existence of fluorescence in Zn:TBP experimentally. A time-averaged photoluminescence spectrum was measured, which confirmed that upon excitation at 532 nm, a fluorescence exists at 658 nm and, to a lesser extent, at 630 nm.* Fluorescence, which allows the excited molecule to de-excite without the release of heat, could contribute to the deviation of our data from the theoretical fit; however, the observed fluorescence does not appear to be strong enough to account for the large deviation in figure 2.

The density change is not instantaneous. It occurs on the order of the speed of sound. What is more, it launches a sound wave that propagates beyond the heated region, so it is a nonlocal event. This additional complication to the analysis is not incorporated into the theory used to derive figure 2. The measured spot size for the limiting performed in figure 2 was $21.4 \mu\text{m}$. Assuming an acoustic velocity typically found in organic solvents of $v \sim 1.5 \times 10^5 \text{ cm/s}$, the acoustic wave generated by the change of density caused by the temperature change will spread to only about half the spot size in 9 ns. Therefore, the heat-generated density change in our model is likely an overestimate, as the experiment was conducted in a transient regime. Since only the centralmost portion of the beam was affected by the thermally induced index change, this arrangement reduced the refractive optical limiting ability of TBP.

* Private conversation with Mary Tobin, ARL, Adelphi, MD.

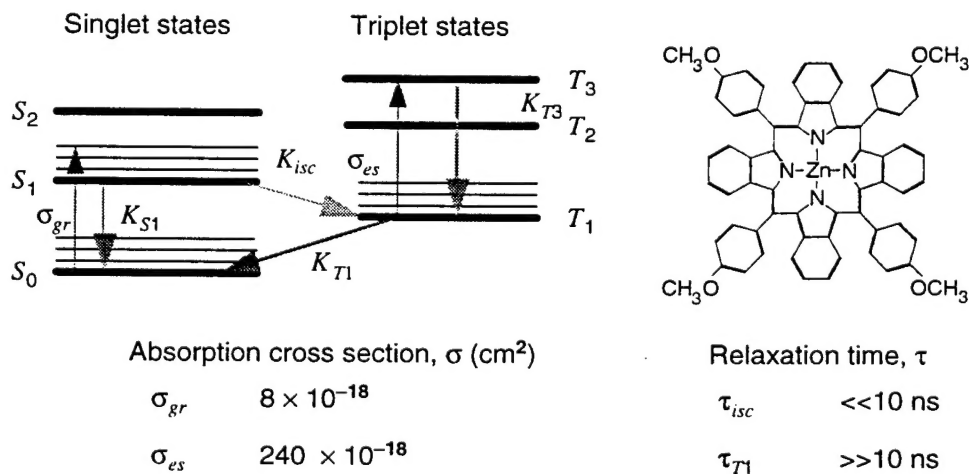
We devised a new experimental arrangement for the limiting experiment with an $f/14$ optical input ($w_o = 4.96 \mu\text{m}$ at focus) to allow the acoustic wave the time to traverse the entire laser beam during the pulse. In this arrangement, the entire thermal response created by the incident laser pulse should enhance the limiting results, and the density change should reach steady state. We used a $100\text{-}\mu\text{m}$ sample length to satisfy the "thin" cell criterion, $L \ll z_o$, that is required for the modeling we employ. In our case, the Rayleigh range, $z_o = \pi w_o^2 / \lambda$, was $141 \mu\text{m}$, where w_o = spot size at focus. In this optical setup, the acoustic wave could fully traverse the laser pulse, but at intensity levels much higher than in the previous experiments.

We performed a Z-scan analysis under the new focusing conditions first to obtain the appropriate parameters for the limiting model [7]. Our work with this material used a Continuum Q-switched, injection-seeded Nd:YAG laser operating at 10 Hz. The laser was frequency doubled to a wavelength of 532 nm and operated in the fundamental transverse electromagnetic (TEM_{00}) mode. We used a dual-leg Z-scan setup to reduce noise in the data. As stated above, the beam radius w_o was $4.96 \mu\text{m}$ at focus. The temporal pulse width at full width at e^{-1} intensity was $\tau_p = 13 \text{ ns}$. To determine the excited-state cross section under our experimental conditions, we assumed a three-level model (fig. 3), with (1) optical transitions from the ground state to the excited singlet state S_1 , (2) intersystem crossing to a triplet state T_1 , and (3) optical transitions from T_1 to an upper level. We also assumed that no measurable saturation or diffusion effects occurred during the pulse, and that the intersystem crossing rate was fast compared to the pulse duration ($\tau_{isc} \ll \tau_p$). Equation (1) describes the change in intensity with distance through the material:

$$\frac{dI}{dz} = -\sigma_{gr} N_{gr}(t)I - \sigma_{es} N_{T1}(t)I, \quad (1)$$

where N_{gr} is the number density of ground state charges, N_{T1} is the number density of charges in the lowest triplet state, the σ 's are the cross sections for absorption in the ground and first triplet state, and I is the beam intensity. Note that this equation assumes that the spot size does not change within the sample; i.e., diffraction is small and ignored. Solving

Figure 3. Three-level model used to describe Zn:TBP. Diagram on right represents a Zn:TBP molecule. Cross sections and relaxation times are given. K 's are decay rates. Subscripts: isc = intersystem crossing; es = excited state; gr = ground, $T1$, $S1$, $T1$, etc. = singlet, triplet states.



this equation for the fluence and energy density, and integrating over the spatial extent of the beam, we may write the normalized energy transmission T through a material of length L as

$$T = \frac{\ln\left(1 + \frac{q_0}{1+x^2}\right)}{\frac{q_0}{1+x^2}}, \quad (2)$$

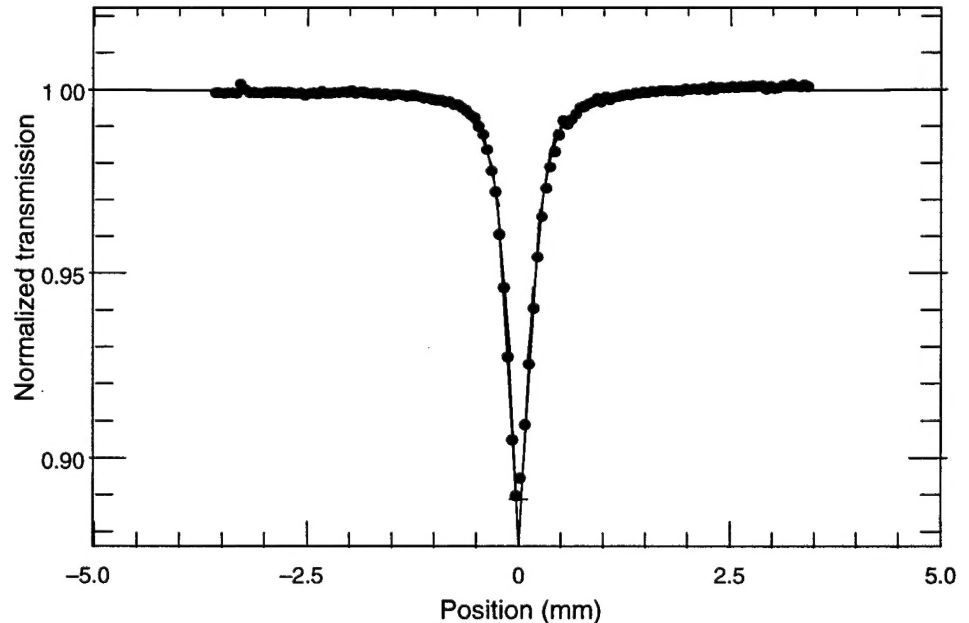
where

$$q_0 = \frac{\Phi(\sigma_{es} - \sigma_{gr})\alpha_0 F_0(r=0)L_{eff}}{2h\omega}, \quad L_{eff} = \frac{1 - e^{-\alpha_0 L}}{\alpha_0},$$

$x = z/z_0$, z is the position of the sample along the optical path ($z = 0$ at focus), $\alpha_0 = \sigma_{gr}N_{gr}(t=0)$, and F_0 is the input fluence as a function of r and position z . The above equation, which assumes an infinite number of charges available in the ground state, can be used to fit the open-apertured Z-scan data and get the value for q_0 . From q_0 , $\Phi\sigma_{es}$ can be obtained, where Φ is the triplet yield and can vary between 0 (no excited charges transfer from the S_1 to T_1 state) and 1 (all the excited charges transfer from the S_1 to T_1 state). A typical open-aperture (where all the transmitted light is collected) Z-scan curve and fit are shown in figure 4.

The apertured Z-scan data contain both the nonlinear absorption and refraction components of the material's nonlinear behavior. Using an aperture that transmits only 25 percent of the beam ($S = 0.25$) in the far field (a distance d from the sample, where $d \gg z_0$), one could iteratively fit the normalized energy transmission to determine the excited-state population refractive index cross section, σ_r , assuming a value for the heat-induced index change. Only two contributions were assumed to add to the nonlinear refraction—one derived from a change in density due to heating of the sample, and the other from the excited-state population contribution to the index.

Figure 4. Typical open-apertured Z-scan. Solid circles represent data and solid line represents a fit using eq (2).



4. Results and Discussion

The open-aperture Z-scan data from the $f/14$ optical setup was fit by equation (2). At energies above 7 nJ, this equation could not exactly fit the data (see fig. 5). Experimentally, the Z-scan curves were wider than expected—i.e., equation (2) predicts a narrower profile based on the measured spot size of the optical system. By varying q_0 in equation (2) to achieve its best fit to the data, we found that the predicted σ_{es} was fluence dependent. As the fluence increased, σ_{es} decreased. At input energies below ~ 1 nJ (2.6 mJ/cm^2), σ_{es} remained constant at the earlier reported value ($\sim 240 \times 10^{-18} \text{ cm}^2$) but with a larger uncertainty. The excited-state cross section should be a constant; therefore its fluence dependence indicates a breakdown in the simple model assumed here, at least above ~ 1 nJ. The most obvious omission was not incorporating saturation of the ground state into the model. If this saturation is incorporated for the fluence, equation (2) becomes

$$\frac{dF}{dz} = -\alpha_0 F_s \left(1 - e^{-F/F_s}\right) - \frac{\sigma_{es} \alpha_0 F_s}{\sigma_{gr}} \left(\frac{F}{F_s} - \left(1 - e^{-F/F_s}\right)\right), \quad (3)$$

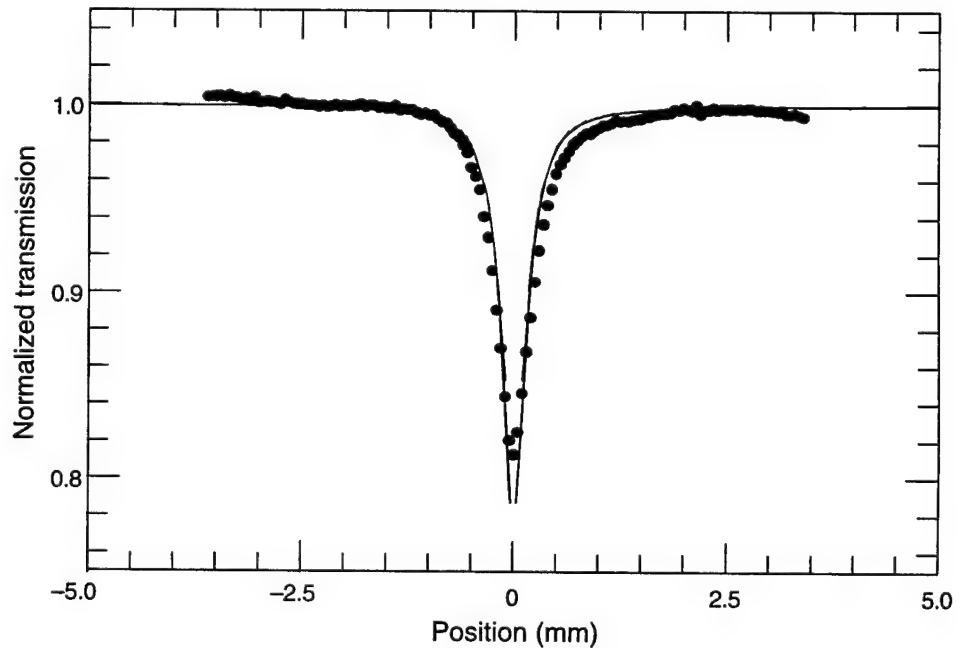
where F_s = saturation fluence, defined as

$$F_s = \frac{h\omega}{\Phi \sigma_{gr}}. \quad (4)$$

Unlike equation (2), this equation cannot be solved in closed form and must be numerically integrated.

While F_s could not be determined exactly because of the uncertainty in the triplet yield, we were confident that the fluences encountered during the optical limiting experiment were well above F_s , which is on the order of

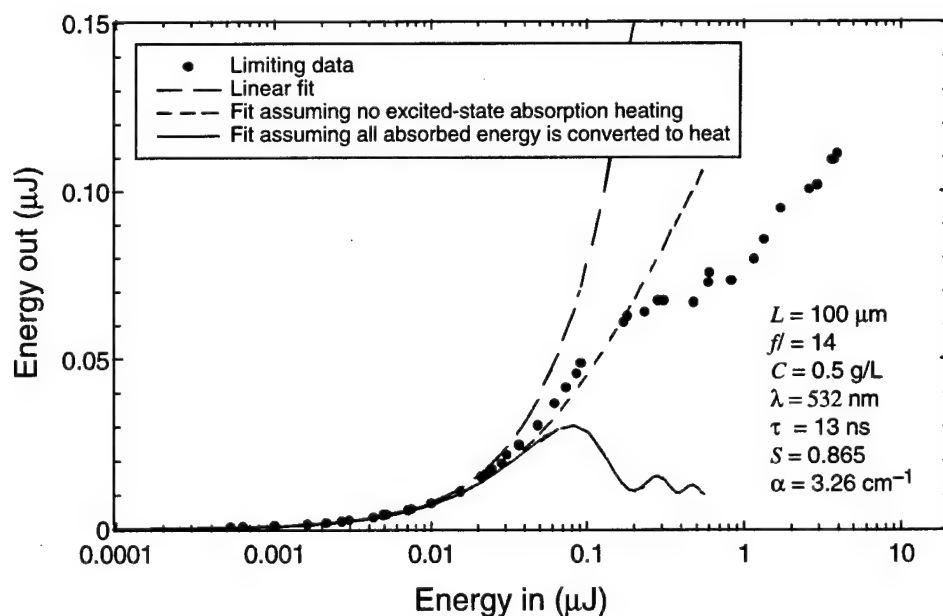
Figure 5. Open-apertured Z-scan for a saturated condition, energy $E = 69 \text{ nJ}$. Solid circles represent data and solid line represents a fit using eq (2).



0.05 to 0.15 J/cm². While adding saturation of the ground state allowed for a more accurate fit, perfect fits to the theory could not be obtained. One possible explanation for this could be triplet-state saturation.

Once again, we performed optical limiting as described above, only using the new $f/14$ optical arrangement. The data and theoretical fits are shown in figure 6. We allowed the heat to fully cross the beam during the pulse over the fluence range that we used in our previous work; however, the limiting curves did not significantly improve. Changing the spot size did not result in the expected thermal contribution, but this could be explained by saturation of the ground state. Saturation prevents the data from limiting as well with increasing input energy for two reasons. First, the absorption does not grow as large as expected; second, the smaller amount of absorption means that the solvent is not heated as much, so that the self-defocusing is not as large. It is interesting to note in figure 6 that limiting above 0.2 μJ is better than would be predicted based on nonlinear absorption and nonlinear refraction, with heat coming only from linear absorption. Since saturation of the absorption most likely is occurring, the absorption does not increase as predicted here, but some heating is occurring from the excited state as well—just not as much as expected based on the unsaturated case. We have not incorporated saturation effects into the limiting model to check this hypothesis but expect to in the near future.

Figure 6. $f/14$ limiter performance.



5. Conclusions

To accurately model this molecule, one cannot ignore saturation effects. In fact, our data indicate that not only is ground-state saturation significant, but saturation of the triplet states may also be occurring. Work is continuing so that we can better understand this behavior and quantify these saturations.

Acknowledgments

We would like to thank Mary Tobin of ARL for performing the fluorescence measurements, Mas Nakashima of Natick Research, Development and Engineering Center for providing the material and helpful discussions, Joe Roach and Barry DeChristofano, also of NRDEC, for general support, and Eric Van Stryland of CREOL for helpful discussions.

References

1. K. Mansour, D. Alvarez, Jr., K. J. Kelly, I. Choong, S. R. Marder, and J. W. Perry, "Dynamics of Optical Limiting in Heavy-Atom Substituted Phthalocyanines," *Organic and Biological Optoelectronics, Proc. SPIE* **1853**, 132–141 (1993).
2. D.V.G.L.N. Rao, F. J. Aranda, J. F. Roach, and D. E. Remy, "Third-Order, Nonlinear Optical Interactions of Some Benzporphyrins," *Appl. Phys. Lett.* **58**, 1241–1243 (1991).
3. S. Guha, K. Kang, P. Porter, J. F. Roach, D. E. Remy, F. J. Aranda, and D.V.G.L.N. Rao, "Third-Order Optical Nonlinearities of Metallotetraporphyrins and a Platinum Poly-ene," *Opt. Lett.* **17**, 264–266 (1992).
4. J. W. Perry, K. Mansour, S. R. Marder, K. J. Perry, D. Alvarez, Jr., and I. Choong, "Enhanced Reverse Saturable Absorption and Optical Limiting in Heavy-Atom-Substituted Phthalocyanines," *Opt. Lett.* **19**, 625–627 (1994) and J. Si, M. Yang, Y. Wang, L. Zhang, C. Li, D. Wang, S. Dong, and W. Sun, "Nonlinear Absorption in Metallo-porphyrin-like Compounds," *Opt. Commun.* **109**, 487–491 (1994).
5. G. L. Wood, M. J. Miller, and A. G. Mott, "Investigation of Tetrabenzporphyrin by the Z-Scan Technique," *Opt. Lett.* **20**, No. 9, 973–975 (1995).
6. G. L. Wood, A. G. Mott, and M. J. Miller, "Nonlinear Optical Properties of Tetrabenzporphyrins," *Mater. Res. Soc. Symp. Proc.* **374**, 267–273 (1995).
7. M. Sheik-bahae, A. A. Said, and E. W. Van Stryland, "High-Sensitivity, Single-Beam n_2 Measurements," *Opt. Lett.* **14**, 955–957 (1990).

Distribution

Admnstr
Defns Techl Info Ctr
Attn DTIC-OCF
8725 John J Kingman Rd Ste 0944
FT Belvoir VA 22060-6218

Army Rsrch Ofc
Attn H Everitt
PO box 12211
Research Triangle Park NC 27709

US Army Matl Cmnd
Asst Dpty CG for RDE Hdqtr
Attn AMCRD COL S Maness
5001 Eisenhower Ave
Alexandria VA 22333-0001

CECOM
Sp & Terrestrial Commctn Div
Attn AMSEL-RD-ST-MC-M H Soicher
FT Monmouth NJ 07703-5203

Dpty Assist Scy for Rsrch & Techl
Attn SARD-TT B Reisman
Attn SARD-TT D Chait
Attn SARD-TT F Milton Rm 3E479
Attn SARD-TT K Kominos
Attn SARD-TT T Killion
The Pentagon
Washington DC 20310-0103

US Army Matl Cmnd
Dpty CG for RDE Hdqtrs
Attn AMCRD BG Beauchamp
5001 Eisenhower Ave
Alexandria VA 22333-0001

Hdqtrs Dept of the Army
Attn DAMO-FDQ D Schmidt
Attn DAMO-FDQ MAJ M McGonagle
400 Army Pentagon
Washington DC 20310-0460

Natick Rsrch and Dev Ctr
Attn SSCNC-IT M Nakashima
Attn SSCNC-IT J Roach
Natick MA 01760-5019

Night Vsn & Elect Sensors Dirctr
Attn AMSEL-RD-NV-STD B Ahn
FT Belvoir VA 22060-5677

ODCSOPS
Attn D Schmidt
Washington DC 20310-1001

OSD
Attn OUSD(A&T)/ODDDR&E(R) J Lupo
The Pentagon
Washington DC 20301-7100

US Army Matl Cmnd
Prin Dpty for Acquisition Hdqtrs
Attn AMCDCG-A D Adams
Attn AMCDCG-T M Fisette
5001 Eisenhower Ave
Alexandria VA 22333-0001

US Army CECOM
Night Vision & Elec Sensors Dir
Attn AMSEL-NV J Pollard
Attn AMSEL-NV J Ratches
10221 Burbeck Rd Ste 430
FT Belvoir VA 22060-5806

US Army Natick Rsrch, Dev, & Engr Ctr
Attn STRNC-YM J Akkara
Natick MA 01760-5020

US Army Rsrch Ofc
Attn AMXRO-PH M Ciftan
PO Box 12211
Research Triangle Park NC 27725

US Army Tank-Automtv & Armaments Cmnd
Attn AMSTA-TR-R-MS-263 R Goedert
Attn AMSTA-TR-R-MS-263 D Templeton
Warren MI 48379-5000

Distribution (cont'd)

US Military Academy
Dept of Mathematical Sci
Attn MAJ D Engen
West Point NY 10996

USAASA
Attn MOAS-AI W Parron
9325 Gunston Rd Ste N319
FT Belvoir VA 22060-5582

Nav Air Warfare Ctr NADC Vision Lab
Attn Code 4.6C-MS-15 J Sheehy
Warminster PA 18974

Nav Rsrch Lab
Attn Code 6656 G Mueller
Attn Code 5613 J Shirk
4555 Overlook Ave SW
Washington DC 20375-5000

WL/MLPH
Attn P Schaefer
Attn C Ristich Bldg 651
3005 P Stret Ste 1B-651
Wright Patterson AFB OH 45433-7702

JPL CA Inst of Techlgy
Attn J Perry
4800 Oak Grove Dr M/S 67-201
Pasadena CA 91109

Natural Sci & Math Complex RM 428
Attn P Prasad
Suny Buffalo
Buffalo NY 14260-3000

Univ of Arkansas Dept of Physics
Attn G Salamo
Fayetteville AR 72701

University of Rochester
Inst of Optics
Attn R Boyd
Rochester NY 14627

Worcester Polytech Inst Dept of Physics
Attn G Swarzlander
100 Institute Rd
Worcester MA 01609-2280

CREOL/UCF
Attn E Van Stryland
PO Box 162700 4000 Central Florida Blvd
Orlando FL 32816-2700

US Army Rsrch Lab
Attn AMSRL-SE H Pollehn
Attn AMSRL-SE-EL A Mott
Attn AMSRL-SE-EL B Ketchel
Attn AMSRL-SE-EL M Miller
10235 Burbeck Rd Ste 110
FT Belvoir VA 22060-5838

US Army Rsrch Lab
Attn AMSRL-CI-LL Tech Lib (3 copies)
Attn AMSRL-CS-AL-TA Mail & Records
Mgmt
Attn AMSRL-CS-AL-TP Techl Pub
(3 copies)
Attn AMSRL-PS-PB M Tobin
Attn AMSRL-SE-E D Wilmot
Attn AMSRL-SE-E J Pellegrino
Attn AMSRL-SE-EO G Wood (5 copies)
Adelphi MD 20783-1197

REPORT DOCUMENTATION PAGE			Form Approved OMB No. 0704-0188	
Public reporting burden for this collection of information is estimated to average 1 hour per response, including the time for reviewing instructions, searching existing data sources, gathering and maintaining the data needed, and completing and reviewing the collection of information. Send comments regarding this burden estimate or any other aspect of this collection of information, including suggestions for reducing this burden, to Washington Headquarters Services, Directorate for Information Operations and Reports, 1215 Jefferson Davis Highway, Suite 1204, Arlington, VA 22202-4302, and to the Office of Management and Budget, Paperwork Reduction Project (0704-0188), Washington, DC 20503.				
1. AGENCY USE ONLY (Leave blank)		2. REPORT DATE January 1998		3. REPORT TYPE AND DATES COVERED Summary, from January 1996 to July 1996
4. TITLE AND SUBTITLE Nonlinear Behavior of Zn:Tetrabenzporphyrin			5. FUNDING NUMBERS DA PR: A31B PE: 611102.31B	
6. AUTHOR(S) Gary L. Wood, Mary J. Miller, and Andrew G. Mott				
7. PERFORMING ORGANIZATION NAME(S) AND ADDRESS(ES) U.S. Army Research Laboratory Attn: AMSRL-SE-EO 2800 Powder Mill Road Adelphi, MD 20783-1197			8. PERFORMING ORGANIZATION REPORT NUMBER ARL-TR-1229	
9. SPONSORING/MONITORING AGENCY NAME(S) AND ADDRESS(ES) U.S. Army Research Laboratory 2800 Powder Mill Road Adelphi, MD 20783-1197			10. SPONSORING/MONITORING AGENCY REPORT NUMBER	
11. SUPPLEMENTARY NOTES AMS code: 61102.A31B ARL PR: 7NE1AA				
12a. DISTRIBUTION/AVAILABILITY STATEMENT Approved for public release; distribution unlimited.			12b. DISTRIBUTION CODE	
13. ABSTRACT (Maximum 200 words) The nonlinear transmission of Zn:tetrabenzporphyrin was measured in a Z-scan setup with 532-nm wavelength laser light and a 13-ns pulse duration. The excited-state absorption cross section, the excited-state refractive index cross section, and the linear and nonlinear absorption contribution to a thermal index change were investigated. The effects of fluorescence and acoustic waves on the nonlinear response of TBP have been determined. Limiter performance was modeled in an f/14 limiter, and saturation effects were identified.				
14. SUBJECT TERMS Nonlinear transmission, porphyrin, z-sacan			15. NUMBER OF PAGES 11	
			16. PRICE CODE	
17. SECURITY CLASSIFICATION OF REPORT Unclassified	18. SECURITY CLASSIFICATION OF THIS PAGE Unclassified	19. SECURITY CLASSIFICATION OF ABSTRACT Unclassified	20. LIMITATION OF ABSTRACT UL	